



Cadmium biosorption by alginate extraction waste and process overview in Life Cycle Assessment context



Emily Nishikawa, Meuris Gurgel Carlos da Silva, Melissa Gurgel Adeodato Vieira*

School of Chemical Engineering, University of Campinas, Cidade Universitária Zeferino Vaz, 13083-852, Campinas, São Paulo, Brazil

ARTICLE INFO

Article history:

Received 5 August 2017

Received in revised form

13 December 2017

Accepted 5 January 2018

Available online 6 January 2018

Keywords:

Biosorption

Cadmium

Sargassum filipendula

Dealginated residue

LCA

ABSTRACT

This work evaluated the cadmium biosorption capacity by the alginate extraction residue from brown seaweed *Sargassum filipendula*, an industry waste which is often discharged into the sea. The biosorption kinetics and equilibrium were investigated, with further analysis of the process thermodynamics. The Mass Transfer in External Film model best described the kinetic data and the rate controlling step is the diffusion through the boundary layer. The kinetic constant values of the model were 0.129, 0.064 and 0.066 1/min for initial concentrations of 1.0, 1.5 and 2.0 mmol/L, respectively. The isotherms were obtained at four temperatures (293, 303, 313 and 323 K) and were analyzed by Langmuir, Freundlich and Dubinin-Radushkevich models. The system was better described by Freundlich model, and the Dubinin-Radushkevich model suggested that the cadmium uptake is of physical nature. The maximum biosorption capacity obtained at 293 and 303 K were 0.394 and 0.429 mmol/g, respectively. The thermodynamic parameters indicated that the biosorption of cadmium is spontaneous and exothermic. The simplified LCA showed that the use of dealginated residue would lead to lower environmental impacts for Acidification, Climate Change, Eutrophication, Human Toxicity and Photochemical Oxidation.

© 2018 Elsevier Ltd. All rights reserved.

1. Introduction

The recent industrial growth has been causing a great impact on ecosystems and on quality of life in cities. Industrial effluents may contain toxic metals, which are hazardous pollutants. They are not easily eliminated from organisms and present potential for biomagnification and bioaccumulation (Barwick and Maher, 2003). Cadmium is a toxic metal largely employed in several processes, including electroplating and pigment production. In human organisms, the presence of cadmium may lead to osteoporosis and damages in kidneys (Åkesson, 2011).

Among the methods for toxic metal removal from effluents, there are chemical precipitation, ion exchange, membrane separation and adsorption (El-Bayaa et al., 2009). Some conventional treatments are expensive and not effective in all range of metal concentration, especially in low concentrations. Membrane

separation, such as reverse osmosis or nanofiltration, may require high pressure leading to a high energy cost (Yang et al., 2014). Chemical precipitation may require a large amount of chemicals to reduce the metal concentration to an acceptable value, resulting in extra cost for sludge disposal and may present difficulties to achieve low concentrations defined by stringent regulations (Kurniawan et al., 2006). In this aspect, biosorption has been increasingly studied for toxic metal removal from aqueous solutions. Alternative and economic materials investigated for cadmium biosorption include agricultural (Basu et al., 2017) wastes, fungal (Ma et al., 2015) and algal (Cardoso et al., 2017b; Fagundes-Klen et al., 2007) biomass.

In biosorption processes, toxic metal ions are passively bound to inactive biomass in aqueous solutions (Davis et al., 2003). Several mechanisms take part in metal binding, such as ion exchange, chelation and physisorption (Volesky and Holan, 1995). For biosorption on seaweeds, ion exchange is reported to be the most relevant mechanism in metal sorption (Davis et al., 2003).

Brown seaweeds are efficient on toxic metal sorption. Furthermore, the biopolymer alginate, present in cell walls of brown seaweeds, is a main responsible for metal binding (Davis et al., 2003). Functional groups of alginate are involved in ion exchange reactions with metal ions, resulting in the uptake of metals from

Abbreviations: D-R, Dubinin-Radushkevich; MTEF, mass transfer in external film; ARE, average relative error; LCA, life cycle assessment; LCIA, life cycle impact assessment; FU, functional unit; AC, activated carbon; AEW, alginate extraction waste.

* Corresponding author.

E-mail address: melissagav@feq.unicamp.br (M.G.A. Vieira).

aqueous phase. *Sargassum filipendula* is a brown algae largely studied: cadmium and zinc in binary system were investigated by Fagundes-Klen et al. (2007); Kleinübing et al. (2013) evaluated the biosorption of lead, copper, cadmium and zinc ions on raw seaweed and on the extracted alginate; Volesky et al. (2003) studied the uptake of copper in a column. On the other hand, brown algae are also raw material for alginate production through extraction, which has applications in food and textile industries (Bertagnolli et al., 2014). In alginate extraction process, it is generated a fibrous residue, which has limited use. This leftover pulp is mainly thrown back into the sea (Kumar and Sahoo, 2017). However, it still contains components of the raw algae and would be employed as a biosorbent of toxic metals (Cardoso et al., 2017a; Costa et al., 2016).

In industry, the use of biosorption is being studied and tested. Michalak et al. (2013) cited two examples of companies offering biosorbents based on algae: Bio-Recovery System (Las Cruces, USA) and B.V. SORBEX (Montreal, Canada). On the other hand, some factors still limit a wider industrial application, such as elevated economic value (Macek and Mackova, 2011). In AEW case, there is not a relevant economic value since it is a residue. However, a limiting factor would be the AEW regeneration for biosorption-desorption cycles in fixed-bed columns for industrial treatment, which is also being studied (Moino et al., 2017).

Life Cycle Assessment (LCA) is a method widely used to evaluate the environmental performance of a product or service (European Commission - Joint Research Centre - Institute for Environment and Sustainability, 2010). Many low cost and alternative materials are investigated for adsorption; however little studies have been conducted to assess the environmental performance of these materials (Dodbiba et al., 2009; Yami et al., 2015).

Therefore, this work aims to investigate the use of the AEW (alginate extraction waste) from the brown seaweed *Sargassum filipendula* as biosorbent for cadmium removal, providing a comprehensive analysis of the kinetics and equilibrium aspects of the cadmium uptake. In addition, the benefits for environment related to the reuse of the AEW are evidenced by the comparison with a commercial adsorbent (AC, activated carbon), in lab scale using the LCA method. The innovative character of this study is the extensive and in-depth investigation of the application of the AEW in toxic metal removal, adding value to the seaweed chain.

2. Material and methods

2.1. Biosorbent material

The brown seaweed *Sargassum filipendula* was collected at São Sebastião (“Cigarras” beach), State of São Paulo, in November of 2015. Costa et al. (2016) characterized the raw seaweed and the residue after alginate extraction.

The raw seaweed presented small diatoms in its structure, similarly as the residue after alginate extraction. In chemical composition, the content of Si decreased due to diatoms release and the content of sodium increased in extraction process. FTIR spectra indicated that the residue maintains functional groups such as carboxylic acids, sulfonate and amino groups, even after alginate extraction, which suggests that AEW has potential to be used as a biosorbent material (Costa et al., 2016).

2.2. Preparation of biosorbent

The seaweed was washed to remove sand and dried in an oven at 60 °C for 24 h. The algae was milled and sieved into fractions smaller than 1 mm. The alginate was then extracted following the method described by Mchugh (1987).

Fifteen g of the raw algae were placed in contact with 500 mL of

an aqueous solution of formaldehyde (0.4% w/w) for 30 min. The algae were rinsed and added to 500 mL of hydrochloric acid solution (0.1 mol/L) for 2 h. Formaldehyde and hydrochloric solutions were applied to clarify the material and remove phenolic compounds. The alginate extraction was performed with 350 mL of a sodium carbonate solution (2% w/v) for 5 h at 60 °C. The mixture was filtered to separate the fibrous residue and the liquid phase with the solubilized alginate. In the presence of sodium carbonate, alginate is converted to a soluble form (Davis et al., 2003) and can be separated from the solid phase.

The AEW was exhaustively washed with deionized water. Ethanol (1:1 v/v) was used for the alginate precipitation. The residue and the precipitated alginate were dried at 60 °C for 24 h. Then, the residue was milled and sieved into fractions with an average diameter of 0.737 mm. The yield of residue and alginate were calculated by Equations (1) and (2).

$$\%Yield (Residue) = \frac{\text{final dry matter of residue}}{\text{seaweed dry matter before extraction}} \cdot 100 \quad (1)$$

$$\%Yield (Alginate) = \frac{\text{final dry matter of alginate}}{\text{seaweed dry matter before extraction}} \cdot 100 \quad (2)$$

2.3. Cadmium solutions

The Cd(II) solutions were prepared by dissolving cadmium nitrate ($\text{Cd}(\text{NO}_3)_2 \cdot 4\text{H}_2\text{O}$), analytical grade (Vetec, Brazil), in deionized water. The pH was adjusted to the required value with nitric acid (0.1 mol/L) solution.

Cadmium concentration was determined by atomic absorption spectrophotometer (AAS) AA-7000, Shimadzu (Japan).

2.4. Biosorption studies

Kinetic (Nishikawa et al., 2016) and equilibrium studies in batch mode were carried out to analyze the sorption of cadmium on the AEW. The biosorbent dose was fixed at 2 g/L and the pH was maintained at 3.5.

In the kinetic study, 500 mL of Cd(II) solutions with three different initial concentrations (1.0, 1.5 and 2.0 mmol/L) were stirred with 1 g of biosorbent at room temperature (20 °C). At predetermined time intervals, solution samples were taken and the residual cadmium concentrations were analyzed by atomic absorption. The Table S4 (Supplementary Material) presents the average results of three measurements and the deviations.

Biosorption isotherms of Cd(II) were obtained through series of 50 mL solutions with different initial concentrations (0.5–18 mmol/L) in capped Erlenmeyer flasks of 100 mL. The bio-adsorbent (0.1 g) was added to each flask and the system was maintained under constant agitation (150 rpm) and temperature (293, 303, 313 and 323 K). The contact time was determined in the kinetic study.

The amount q of metal adsorbed (mmol/g) and the removal percentage (%Rem) were calculated from the Equations (3) and (4):

$$q = (C_0 - C_e) V / m \quad (3)$$

$$\%Rem = C_0 - C_e / C_0 \cdot 100 \quad (4)$$

where: V is the volume of solution (L), m is the mass of dry

biosorbent (g), C_0 and C_e are the initial and equilibrium concentrations of cadmium (mmol/L), respectively.

2.5. LCA methodology

2.5.1. Goal and scope definition

The goal of this study is to compare the environmental performance of AEW and AC. The results are intended to reveal if the employment of AEW would result in environmental gain. The functional unit was the adsorbent mass required to reduce the cadmium concentration of 1 L of wastewater from 0.05 mg/L, a typical final value of precipitation (Metcalf and Eddy, 2015), to 0.001 mg/L (standard value in Brazil).

The scope involves the production, transportation, use and waste management phases. During the use phase, it was assumed a batch process for adsorption at room temperature (20 °C). For waste treatment, it was considered that the particles were calcined for 5 h and sent to a hazardous material landfill.

Fig. 1 presents the processes included. Alginate extraction phase was not included in the study.

2.5.2. Life cycle inventory

For AC production, overseas transport, electricity and landfill, Ecoinvent Database v.3 was used. The adsorbent required mass for the treatment was calculated using the maximum adsorption capacity parameter, provided by Langmuir isotherm, described in Equation (15). This parameter provides the maximum amount of cadmium adsorbed by a unit mass of the adsorbent. For AC, the adsorption capacity was obtained from the work of Asuquo et al. (2017). For AEW, the adsorption capacity was obtained from laboratory experiments.

Considering the cadmium concentration decrease from 0.05 mg/L to 0.001 mg/L, the required mass of each adsorbent was calculated (Supplementary Material). Table 1 lists the information of each system.

2.5.3. AC inventory

The AC was produced in Europe (Wernet et al., 2016) and the

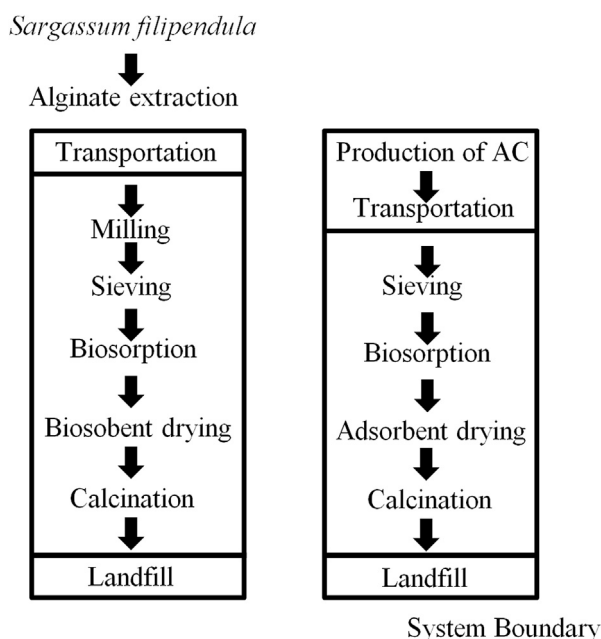


Fig. 1. System boundary of the biosorption process analyzed in LCA.

Table 1

Adsorption process information for AC and AEW.

Adsorbent	AC	AEW
Time for removal (h)	3 ^a	2.5 ^b
Adsorption capacity (mmol/g)	0.24 ^a	0.39 ^b
Required mass (mg)	1.82	1.12

^a Asuquo et al. (2017).

^b Laboratory data. The values are listed in Section 4.1 and Table 3.

transport was considered from Germany to Brazil, corresponding to 13,012 km.

2.5.4. AEW inventory

Tuazon and Corder (2008) discussed the allocation aspect in the reuse of wastes (red mud). They assumed it was reasonable to consider the red mud “free of charge” since it was not the primary goal of the production process. AEW is not the primary goal of the production process and, in addition, according to Kumar and Sahoo (2017), AEW is generally discarded in the sea. This fact could cause other environmental impacts, but for this study, this residue was only considered a raw material, with no inherent value or impact. Therefore, allocation factors were not considered.

For the transportation to Brazil, the origin of the AEW was considered to be India, which is a country that processes the seaweed investigated in this study (Mchugh, 1987). The distance corresponds to 17,690 km.

The alginate manufacturing facility was assumed to be close to the port, therefore the transportation within India was not considered. Also, the land transportation within Brazil was not considered because this work aims to compare two options; the land transportation would be the same for AC and AEW, and would not affect the final result.

2.5.5. Electricity inventory

For the adsorption process, the energy demands were computed based on the equipments of the laboratory (Table S1, Supplementary Material). In the use phase of AC, it was considered that the particles were sieved before the adsorption. For the AEW, the particles were first milled and then sieved. In both cases, an oven was used to dry the adsorbents after use and a furnace was used to calcine the adsorbents for 6 h. The sieving step was not considered due to the scale of this study and consequent difficulty to observe the difference between the sift processes. Also, the calcination process was the same for AEW and AC, according to the procedure followed (Díaz-Vázquez et al., 2015); therefore, it was not considered in the inventory.

The Brazilian electricity mix is shown in Table S2 (Supplementary material) (EPE, 2017). An alternative case regarding the mix planned for 2024 was also analyzed to observe the effects of a more renewable mix on the results (EPE and MME, 2015).

The OpenLCA 1.4.2 software (Green Delta, 2015) was employed to perform the impact assessment and Table S3 (Supplementary Material) summarizes the inventory for AC and AEW.

2.5.6. Impact assessment methods and impact categories

The method used for the impact assessment step was the CML (Guinée et al., 2002). The midpoint impact categories considered were: Acidification (ACID), Climate Change (CC), Human Toxicity (HT), Photochemical Oxidation (PO) and Eutrophication (EUTR).

2.5.7. General assumptions

The adsorbent mass losses during the process were not considered. The facilities and equipments in the use and waste

Table 2
Kinetic parameters for cadmium biosorption on the AEW from *Sargassum filipendula*.

		Initial concentration of Cd(II)		
		1.0 mmol/L	1.5 mmol/L	2.0 mmol/L
Pseudo first order	q_e (mmol/g)	0.338	0.388	0.701
	k_1 (1/min)	0.229	0.148	0.090
	R^2	0.924	0.978	0.993
	ARE (%)	10.43	11.54	3.69
Pseudo second order	q_e (mmol/g)	0.352	0.405	0.743
	k_2 (g/mmol.min)	1.136	0.594	0.185
	R^2	0.953	0.958	0.974
	ARE (%)	8.25	14.45	10.90
MTEF	K_{TM} (1/min)	0.129	0.064	0.066
	R^2	0.969	0.990	0.997
	ARE (%)	11.11	11.03	4.88
	c (mmol/g)	0.033	-0.009	-0.062
Intra-particle diffusion	k_i (mmol/g.min ^{1/2})	0.073	0.090	0.144
	R^2	0.866	0.946	0.966
	ARE (%)	14.78	24.29	509.45
	D_i (cm ² /min)	$8.451 \cdot 10^{-5}$	$6.303 \cdot 10^{-5}$	$5.792 \cdot 10^{-5}$
Boyd	R^2	0.985	0.931	0.983

Table 3
Equilibrium parameters obtained from Langmuir, Freundlich and D-R models for cadmium biosorption on the AEW at different temperatures.

Model	Parameter	Temperature			
		293 K	303 K	313 K	323 K
Langmuir	q_{max} (mmol/g)	0.394	0.429	0.333	0.824
	K_L (L/mmol)	0.354	2.186	1.932	0.483
	R_L	0.209	0.456	0.529	0.787
	R^2	0.927	0.911	0.947	0.958
	ARE (%)	20.89	18.10	17.78	23.50
Freundlich	K_F (mmol ^{1-1/n} .L ^{1/n} /g)	0.133	0.251	0.191	0.257
	n	2.295	4.125	3.805	2.201
	R^2	0.947	0.780	0.971	0.993
	ARE (%)	16.44	20.78	7.07	5.68
	q_{max} (mmol/g)	0.286	0.397	0.286	0.607
D-R	$k \cdot 10^8$ (mol ² /J)	2.761	6.779	4.737	14.088
	E (kJ/mol)	4.255	2.716	3.249	1.884
	R^2	0.825	0.856	0.801	0.845
	ARE (%)	29.15	21.06	24.76	34.84
	Experimental	q_m (mmol/g)	0.352	0.397	0.336

management phases were considered the same for both cases (AC and AEW); therefore they were not included.

Regeneration of adsorbents was not considered due to lack of data. For pH control in AEW process, it was considered the addition of nitric acid.

For calcination, the AC was considered to have 3.5% of ash (Wernet et al., 2016) and the rest would be emitted as CO₂. For AEW, the ash content of 6% was determined in the laboratory following the procedure reported by Díaz-Vázquez et al. (2015). The nitrogen and carbon content was considered 1.5% and 30% (Cruz-Rivera and Hay, 2001), respectively. During calcination, nitrogen was emitted as NO₂ and carbon as CO₂.

3. Theory and calculation

Kinetic modeling of the process gives information about the adsorption rate and controlling step of the process. Adsorption kinetic models may describe the process as a chemical reaction or as sequence of diffusion steps and a final adsorption step (Qiu et al., 2009). Pseudo-first and pseudo-second order models are based on a chemical reaction consideration and provide overall rates of adsorption, from a global perspective. On the other hand, diffusion models consider different steps in the process and it is possible to verify which one is rate limiting. Intra-particle diffusion, Boyd and

mass transfer in external film (MTEF) are examples of diffusion models.

In this study, pseudo-first order, pseudo-second order, intra-particle diffusion, Boyd and resistance to mass transfer in external film were used to describe the adsorption kinetics.

For the first order sorption (Ho, 2004):

$$\frac{\partial q}{\partial t} = k_1(q_e - q) \quad (5)$$

Integrating this for boundary conditions $t = 0$ to $t = t$ and $q = 0$ to $q = q_e$, gives:

$$q = q_e(1 - e^{-k_1 t}) \quad (6)$$

where: q_e is the amount of cadmium adsorbed at equilibrium (mmol/g), q is the amount of cadmium adsorbed at time t (mmol/g), k_1 is the pseudo-first order constant (1/min).

For the rate constant of pseudo-second order (Ho and McKay, 1999):

$$\frac{\partial q}{\partial t} = k_2(q_e - q)^2 \quad (7)$$

Integrating this for boundary conditions $t = 0$ to $t = t$ and $q = 0$ to $q = q_e$, gives:

$$\frac{q}{q_e} = \frac{k_2 q_e t}{1 + k_2 q_e t} \quad (8)$$

where: k_2 is the pseudo-second order rate constant (g/mmol.min).

Adsorption rate may be controlled by intra-particle diffusion or by mass transfer through the external (boundary) film (Khezami and Capart, 2005). Thus, in order to determine the rate controlling step, the results were fitted to the Intra-particle Diffusion, Boyd and Resistance to Mass Transfer in External Film models.

Intra-particle diffusion model (Weber and Morris, 1963) is formulated as:

$$q = k_{di} \cdot t^{1/2} + c \quad (9)$$

where: k_{di} (mmol.g.min^{0.5}) is the intra-particle diffusion rate constant and c (mmol/g) is a constant related to the thickness of the boundary layer. The value of constant c provides information about the magnitude of the resistance to external mass transfer (Khezami

and Capart, 2005).

Boyd model (Boyd et al., 1947) also considers intra-particle diffusion and can be described by:

$$F = \frac{q}{q_e} = 1 - \frac{6}{\pi^2} \exp(-B_t) \quad (10)$$

where: F is the fractional equilibrium achieved at time t, and B_t is a parameter, function of F according to Equation (11):

$$B_t = -0.4977 - \ln(1 - F) \quad (11)$$

Thus, B_t is calculated for each value of F, then it can be plotted against t. In case of a linear behavior with the plot passing through the origin, intra-particle diffusion is the rate controlling step. Otherwise, the external mass transfer is the limiting process (El-Khaiary, 2007). Another result given by this model is the effective diffusion coefficient D_i (cm^2/s), obtained from the angular coefficient α of the plot of B_t against t.

$$\alpha = \frac{D_i \pi^2}{r_0^2} \quad (12)$$

where: r_0 is the radius (cm) of the biosorbent assuming a spherical shape.

The MTEF model (Puranik et al., 1999) assumes that the diffusion through the boundary layer is the limiting step. Other assumptions are: intra-particle diffusion is negligible, the adsorbent surface is spherical and homogeneous, perfect mixing in reaction volume, equilibrium between the solute and the interface (on particle surface) is reached rapidly, volume and temperature are constants (Puranik et al., 1999). The MTEF model can be written as follows (Cantuaria et al., 2016):

$$\frac{dq}{dt} = \frac{V}{m} K_{MT} [C(t) - C_i(t)] \quad (13)$$

where: C is the solution concentration (mmol/L) at time t, V is the volume of solution (L), m is the mass of adsorbent (g), K_{MT} is the external film mass transfer coefficient (1/min), C_i is the concentration of solute in the boundary layer (mmol/L).

The Langmuir, Freundlich and Dubinin-Radushkevich (D-R) models were fitted to equilibrium data by non-linear regression. Langmuir (1918) model assumes the adsorption of one adsorbate molecule by active site (monolayer adsorption) and also assumes that all sorption sites are energetically uniform (Ruthven, 1984). The Langmuir isotherm is given by the following equation:

$$q = \frac{q_{max} \cdot K_L \cdot C_e}{1 + K_L \cdot C_e} \quad (14)$$

where: q_{max} is the maximum metal sorption capacity (mmol/g), K_L is the ratio between adsorption and desorption rates (L/mmol) and C_e is the equilibrium concentration of cadmium (mmol/L).

Hall et al. (1966) suggested the calculation of a dimensionless equilibrium parameter named R_L . This parameter gives information about the favorability of the isotherm, according to Equation (15). This parameter is null for irreversible isotherms, falls in the range of 0–1 for favorable cases and R_L is higher than 1 in non-favorable isotherms.

$$R_L = \frac{1}{1 + K_L C_0} \quad (15)$$

where: C_0 is the initial concentration of the adsorbate in the aqueous phase (mmol/L).

Freundlich model considers a multilayer adsorption, the heterogeneity of adsorbent particles and is described by (Davis et al., 2003):

$$q = K_F \cdot C_e^{1/n} \quad (16)$$

where: K_F ($\text{mmol}^{1-1/n} \cdot \text{L}^{1/n}/\text{g}$) and n are constants. The values of K_F and n are related to the uptake intensity and to the maximum adsorption capacity, respectively.

D-R isotherm (Dubinin and Radushkevich, 1947) is more general than Langmuir model in the sense that it does not assume a homogeneous surface (Aksoyoglu, 1989; Inyınbor et al., 2016). This model also provides an insight on the type of adsorption, physical or chemical (Baláz et al., 2015; Chakravarty et al., 2010). The isotherm is expressed by:

$$\ln(q) = \ln(q_{max}) - k\varepsilon^2 \quad (17)$$

where: q is the amount of cadmium adsorbed per unit weight of adsorbent (mmol/g), q_{max} is the maximum adsorption capacity (mmol/g), k is the constant related to the sorption energy (mol^2/J^2) and ε is the Polanyi potential, which is given by:

$$\varepsilon = RT \ln \left(1 + \frac{1}{C_e} \right) \quad (18)$$

where: R is the gas constant (J/mol.K) and T is the temperature (K).

The parameters of the model can be calculated from the intercept and slope of the plot of $\ln(q)$ versus ε^2 . The mean energy of sorption E (kJ/mol) is calculated by Equation (19). Values between 1 and 8 kJ/mol indicate a physisorption, while energies between 9 and 16 kJ/mol are characteristic of chemisorption (Chakravarty et al., 2010; Jain et al., 2009).

$$E = \frac{1}{\sqrt{2k}} \quad (19)$$

The thermodynamic parameters were calculated using the Freundlich constant obtained at the temperatures of the isotherms. Usually, constants of Henry, Langmuir or other isotherms are employed (Ghosal and Gupta, 2015; Tran et al., 2016). However, in this case, Freundlich model presented the best fit to the equilibrium data. In order to maintain the consistency of units, Equation (20) (Tran et al., 2016) was applied to convert the unit of K_F , while Equation (21) (Ghosal and Gupta, 2015) was applied to obtain the dimensionless equilibrium constant K_{eq} .

$$K'_F \left[\frac{\text{mg}}{\text{g}} \frac{\text{L}^{1/n}}{\text{mg}^{1/n}} \right] = K_F \left[\frac{\text{mmol}}{\text{g}} \frac{\text{L}^{1/n}}{\text{mmol}^{1/n}} \right] (M_{Cd})^{1-\frac{1}{n}} \quad (20)$$

$$K_{eq} = K'_F \rho \left(\frac{1}{\rho/1000} \right)^{\left(1-\frac{1}{n} \right)} \quad (21)$$

where: K_F ($\text{mmol} \cdot \text{L}^{1/n}/\text{g} \cdot \text{mmol}^{1/n}$) and n are the Freundlich constants obtained from the equilibrium isotherm, K'_F ($\text{mg} \cdot \text{L}^{1/n}/\text{g} \cdot \text{mg}^{1/n}$) is the modified Freundlich constant, M_{Cd} is the molecular weight of the adsorbate (mg/mmol) and ρ (g/L) is the mass of water per liter at the temperature of the isotherm.

The thermodynamics of the sorption process was analyzed by the calculation of the enthalpy (ΔH), entropy (ΔS) and the Gibbs energy (ΔG) changes using Equations (22) and (23) (Adebisi et al., 2017; Demiral and Güngör, 2016).

$$\ln K_{eq} = -\frac{\Delta H}{RT} + \frac{\Delta S}{R} \quad (22)$$

$$\Delta G = -RT \ln K_{eq} \quad (23)$$

4. Results and discussion

The yield of alginate extraction from *Sargassum filipendula* was $24 \pm 5\%$. This result is in agreement with the alginate content of brown seaweeds (10–40%) reported in the literature (Davis et al., 2003; Kleinübing et al., 2013). The yield of the biosorbent used in this study (AEW) was $52 \pm 3\%$. It is possible to conclude from the high percentage of residue that alginate production generates a large amount of waste. Therefore, this material would be of great interest in toxic metal removal.

4.1. Sorption kinetics

Fig. 2 shows the kinetic curves obtained for biosorption of Cd(II) in the three initial concentrations tested.

At 150 min, the system is already in equilibrium with adsorbed amounts q_e of 0.34, 0.38 and 0.69 mmol/g for the concentrations of 1.0, 1.5 and 2.0 mmol/L, respectively. These values correspond to 57%, 42% and 54% of removal, respectively. Thus, the adsorbed amounts increased with an increase in initial concentration due to the higher driving force for mass transfer, same behavior verified by Esmaeili et al. (2015) for the biosorption of mercury on algae *Sargassum glaucescens*. Also, Romero-González et al. (2001) investigated the cadmium uptake by a commercial residue of alginate extraction (from a mix of seaweeds) and obtained 0.37 and 0.59 mmol/g of removal for initial concentrations of 1.0 and 2.0 mmol/L, respectively, similar result of this work.

Table 2 shows the parameters obtained in non-linear kinetic modeling. The validity of the applied models was evaluated by the correlation coefficients (R^2) and the average relative error (ARE).

Pseudo-first order model was more predictive than pseudo-second order model, as indicated by the values of R^2 , ARE and the proximity between experimental and calculated values of q_e . In this case, the concentration in the saturation state is proportional to the

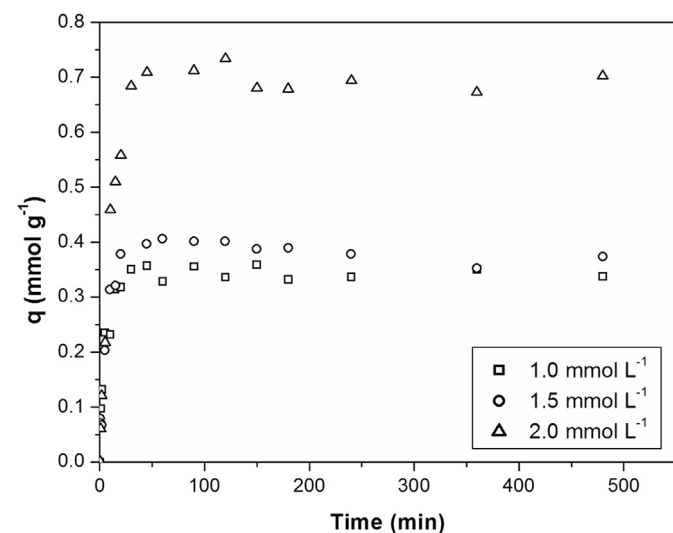


Fig. 2. Kinetic curves for cadmium biosorption on the AEW with cadmium initial concentrations of 1.0, 1.5 and 2.0 mmol/L.

adsorbed amount (Ben-Ali et al., 2017) and the adsorption rate is directly related to the total unoccupied sites (Blázquez et al., 2011). At low concentrations, the number of available binding sites is higher; therefore the adsorption is faster in comparison to experiments at higher concentrations. It results in the decrease in rate constants with the increase in initial cadmium concentration. The same observation was made by Ebrahimi et al. (2015) for cadmium biosorption on a shrub plant seed.

In regard to the adsorption mechanism, intra-particle diffusion, Boyd and MTEF models were applied to the data. In Table 2 it can be seen that the intercepts (parameter c, according to Equation (9)) of the plots q vs. $t^{1/2}$ of Intra-particle diffusion model were close to, but not zero. According to this model, intra-particle is the limiting step if the line passes through the origin and if the plot is linear. Hence, the result suggests that internal diffusion is not determinant to adsorption rate.

The Boyd model resulted in curves which did not cross the origin. Thus, according to the model (El-Khaiary, 2007), intra-particle diffusion is not the rate controlling step. In addition, the effective diffusion coefficient D , obtained by Boyd model were four to five orders of magnitude higher than 10^{-10} cm²/min, which according to Singh et al. (2005) is the value for cases with intra-particle diffusion controlling step.

The correlation coefficients of intra-particle diffusion model did not indicate a good adjustment, with a R^2 of 0.866 for the concentration of 1.0 mmol/L. However, the results agree with the findings obtained with Boyd model, indicating that internal diffusion does not control the adsorption rate. Therefore, MTEF model, which assumes that film diffusion is rate limiting, was employed.

MTEF correlation coefficients were higher and ARE were lower than for other models. This fact corroborates the conclusion that the diffusion through the boundary layer is the rate controlling step of cadmium biosorption on dealginate residue from *Sargassum filipendula*. Thus, an increase in agitation should reduce the mass transfer resistance (Leusch and Volesky, 1995).

4.2. Equilibrium isotherms

Fig. 3 shows the isotherms for biosorption of Cd(II) on the AEW obtained in 293, 303, 313 and 323 K. The maximum biosorbed amount and the parameters obtained from model fittings are listed in Table 3. In general, the isotherms present characteristic shapes of favorable isotherms (McCabe et al., 2001).

From Table 3, in relation to R^2 and ARE, Freundlich model best described the biosorption of Cd(II) on the residue, except for the temperature of 303 K. However, at 303 K, the ARE values for Langmuir and Freundlich are close (18.10 and 20.78%, respectively). Therefore, Freundlich model was considered to best fit the equilibrium data. Past studies verified that Freundlich model describes the biosorption of toxic metals on the raw algae *Sargassum filipendula*. Vieira et al. (2007) investigated the biosorption of lead and Fagundes-Klen et al. (2007) studied the removal of cadmium and zinc, both works applied the seaweed *Sargassum filipendula*.

On the other hand, D-R model did not fit well the data and its results may only represent an estimate. Nevertheless, the energy values (E) obtained were lower than 8 kJ/mol, indicating that the biosorption of cadmium on AEW is physical in nature. Plaza Cazón et al. (2012) and Vilar et al. (2006) also verified a physical biosorption of cadmium on seaweeds *Macrocystis pyrifera* e *Gelidium*, respectively.

The parameter n from Freundlich model resulted in values between 1 and 10. In addition, the values of R_L parameter from Langmuir isotherm were lower than 1. Both parameters denote a favorable biosorption (Adebisi et al., 2017; Hall et al., 1966).

In regard to Langmuir isotherm, at the highest temperature

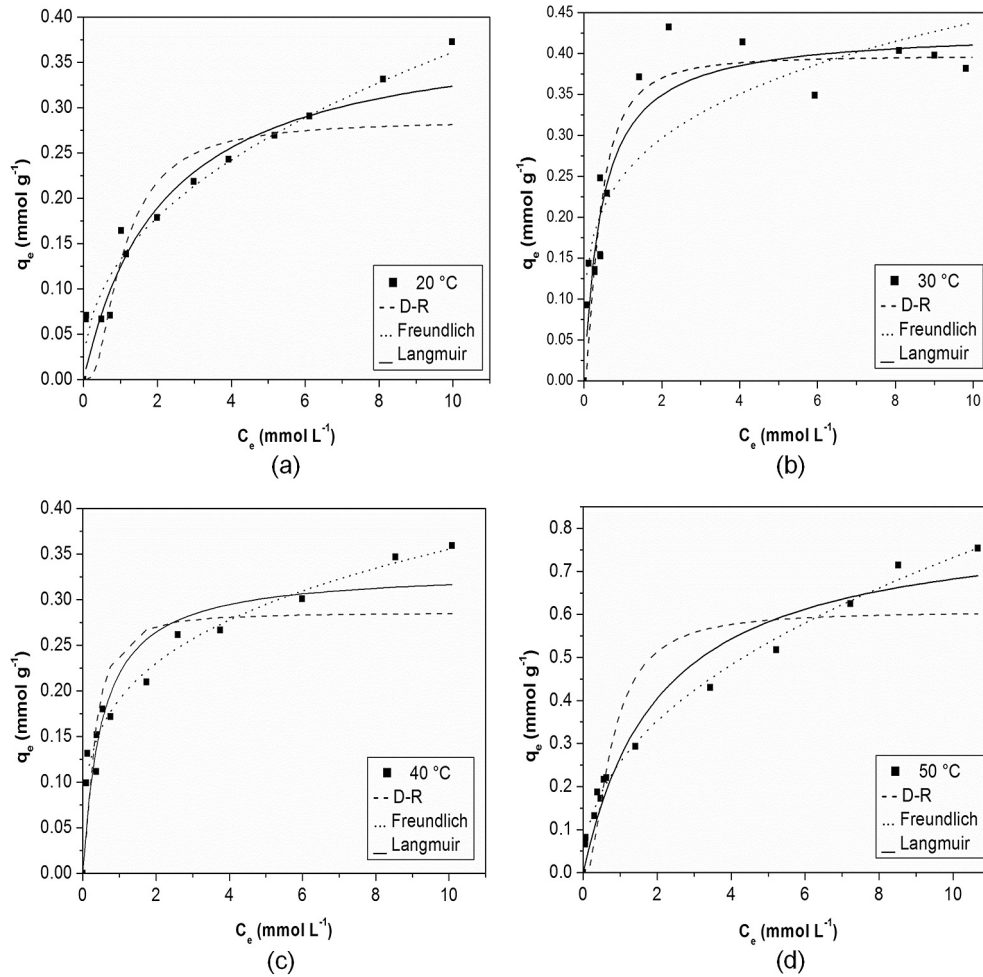


Fig. 3. Biosorption isotherms for Cd(II) biosorption on the AEW at (a) 293 K (20 °C); (b) 303 K (30 °C); (c) 313 K (40 °C) and (d) 323 K (50 °C).

studied, it was obtained the highest amount of Cd(II) adsorbed. Moreover, [Fagundes-Klen et al. \(2007\)](#) reported a q_{\max} of 0.63 mmol/g at 303 K for the seaweed *Sargassum filipendula* “in natura”. Therefore, even after alginate extraction, the algal residue maintains more than 50% of *Sargassum filipendula* biosorption capacity.

[Table 4](#) presents q_{\max} values obtained by Langmuir model for various seaweeds in cadmium biosorption. It is possible to verify that the AEW maintains an interesting cadmium biosorption capacity compared to other materials.

4.3. Thermodynamic study

The values of K_F from [Table 3](#) were used to calculate the equilibrium constant K_{eq} , for subsequent calculation of thermodynamic parameters ΔH , ΔS and ΔG . [Table 5](#) lists the thermodynamic parameters obtained.

Table 4

Maximum cadmium biosorption capacities for seaweeds reported in the literature.

Seaweed	q_{\max} (mmol/g)	Temperature (K)	pH	Reference
<i>Sargassum filipendula</i>	0.63	303	5.0	Fagundes-Klen et al. (2007)
<i>Padina sp.</i>	0.53	298	5.0	Kaewsarn and Yu, (2001)
<i>Fucus vesiculosus</i>	0.65	299	3.5	Holan et al. (1993)
AEW from <i>Sargassum filipendula</i>	0.43	303	3.5	This study

Table 5

Thermodynamic parameters for the biosorption of cadmium on the AEW.

Parameter	Temperature		
	303 K	313 K	323 K
K_F (mg/g) ($L^{1/n} \cdot mg^{1/n}$)	8.972	6.026	3.383
K_{eq}	9001.87	6060.94	3404.68
ΔG (kJ/mol)	-22.94	-22.66	-21.84
ΔH (kJ/mol)	-39.61		
ΔS (J/mol.K)	-54.26		

The negative values of ΔG indicate that the biosorption of cadmium on the AEW from *Sargassum filipendula* is spontaneous. [Bertagnolli et al. \(2014\)](#) also verified the spontaneity of chromium sorption on the same biosorbent of this study. Values of ΔG ranging from -400 to -80 kJ/mol indicate chemisorption, while values from -20 to 0 kJ/mol are characteristics of physisorption ([Yu et al.](#),

Table 6
Life cycle impact assessment of AEW and AC.

Impact category	AC	AEW
Acidification (kgSO ₂ Eq)	1.21.10 ⁻⁰³	1.05.10 ⁻⁰³
Climate Change (kgCO ₂ -Eq)	3.03.10 ⁻⁰¹	2.63.10 ⁻⁰¹
Human Toxicity (kg1,4-DCB-Eq)	2.63.10 ⁻⁰²	2.29.10 ⁻⁰²
Eutrophication (kgPO ₄ ³⁻ -Eq)	1.21.10 ⁻⁰⁴	1.13.10 ⁻⁰⁴
Photochemical Oxidation (kgEthylene-Eq.)	4.76.10 ⁻⁰⁵	4.14.10 ⁻⁰⁵

2001). In this study, the results were close to the range indicative of physisorption, supporting the inference from D-R isotherm analysis.

It was obtained a negative variation in enthalpy, indicating that the biosorption is exothermic. However, the biosorption capacity increased with increasing temperature, as can be seen in Table 3. This behavior may be related to the ion exchange mechanism and may be an indicative of its role in the process. At higher temperatures, the mobility of ions increases (Mobtaker et al., 2008), favoring the uptake of metal ions. Bertagnolli et al. (2014) also verified a negative ΔH and an increase in biosorption capacity with increasing temperature.

The negative values of ΔS signify that the entropy decreases in the process. Bertagnolli et al. (2014) also observed negative values for ΔG , ΔH and ΔS parameters for chromium biosorption on the same biosorbent of this study.

4.4. Life cycle assessment

The comparison between the use of AC and AEW is presented in

Table 6 and Fig. 4 presents the relative results. It is possible to verify that the AEW option resulted in smaller impacts.

For AC and AEW, electricity consumption accounts for most part of impacts (Fig. 4a). The pH control is relevant for EUTR in AEW case due to the need of nitric acid for pH control.

In the electricity mix, the technology with the highest impact was the oil-fired thermal power, even with only a share of 3.7%. It represented 60% of the electricity impact in HT, 50% in ACID, 45% in PO, 20% in CC and EUTR. Coal-based power (share of 2.9%) was also relevant for ACID (24%), HT (24%) and PO (21%). Thermal power from biomass (especially sugarcane) is another important source with impacts in ACID (23%) and EUTR (60%), mainly due to fertilizer use. The major technology in Brazilian mix is hydroelectricity (share of 68.1%). It accounted for 23% of impacts in CC due to CO₂ and CH₄ emissions related to land transformation, and 20% in PO due to biogenic CH₄.

Fig. 4b and c depict the contribution of each sub-process except electricity consumption. For ACID, CC, HT and PO categories, the AC production and calcination are relevant steps for AC and AEW, respectively. The AEW option avoids AC production, which encompasses electricity consumption, hard coal and natural gas burning (Wernet et al., 2016) (Fig. S1 in Supplementary Material).

Fig. 5 shows the comparison between the base case and the alternative scenario (2024 electricity mix).

The alternative case resulted in a profile similar to the obtained for the base case except for EUTR. The reduction of 2.4% in non-renewable sources resulted in impact reductions of more than 5% in all categories, exception for EUTR. In this case, the impacts related to biomass-derived electricity overcome the lower impacts

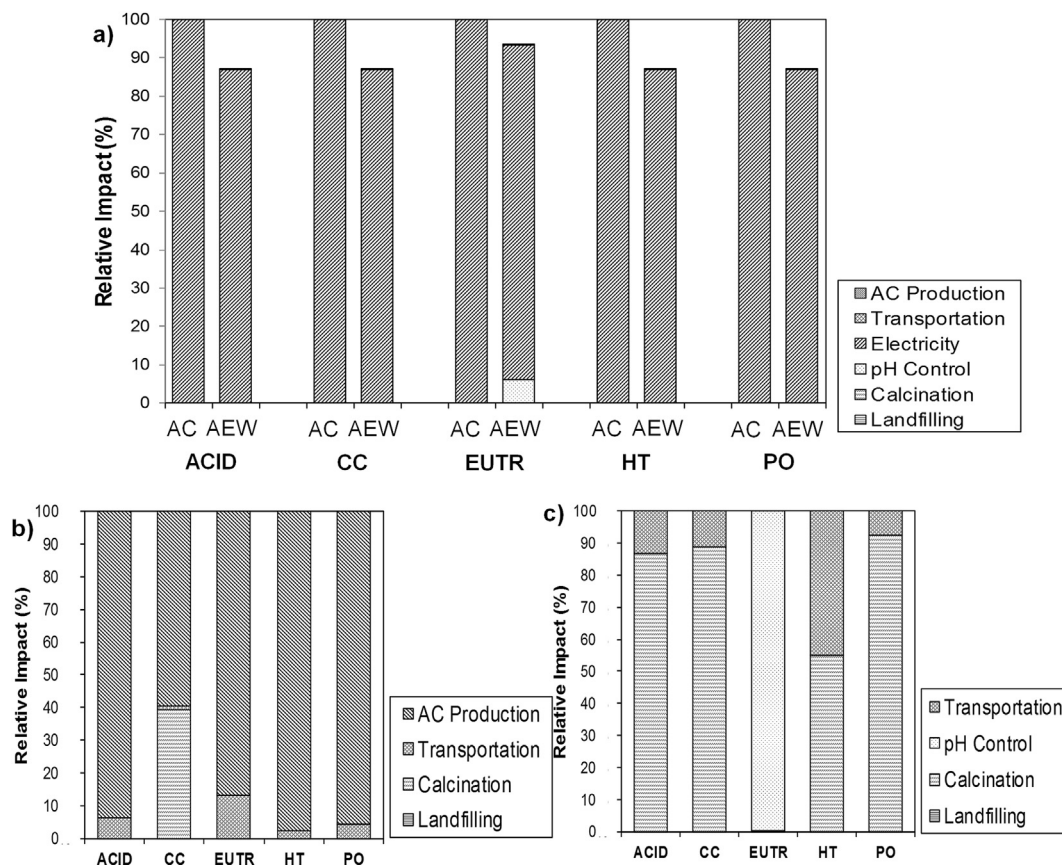


Fig. 4. Comparison between AC and AEW use. (a) Considering electricity (b) AC without electricity (c) AEW without electricity. The maximum result of each category was considered to be 100%.

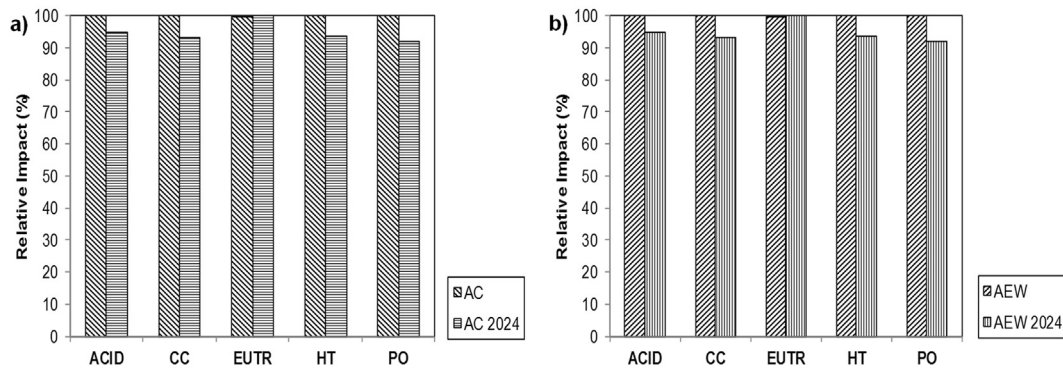


Fig. 5. Comparison between Base and Alternative Cases (a) AC and (b) AEW. The maximum result of each category was considered to be 100%.

related to the other technologies in the mix. For AC, the biomass-derived electricity accounted for 61.5% of EUTR impacts in base case and increased to 65% in alternative case. For AEW, it increased from 57.4% (base case) to 60.6% (alternative case).

5. Conclusions

The results obtained in this study demonstrated that the residue of alginate extraction from the brown seaweed *Sargassum filipendula* is a promising biosorbent material for cadmium removal from aqueous solutions. The equilibrium is established rapidly, within 150 min, and the rate controlling step is the diffusion through the boundary layer. Pseudo-first order and MTEF models were the most predictive for kinetic data. The shapes of the isotherms indicate a favorable biosorption and the Freundlich model described the equilibrium data. The dealginated residue presented an interesting cadmium biosorption capacity of 0.43 mmol/g (at 303 K) in comparison with other raw seaweeds. The negative values of ΔG and ΔH indicated that Cd(II) biosorption is spontaneous and exothermic.

LCA analysis showed that the use of AEW resulted in lower impacts in all categories. Electricity is a hotspot and a more renewable mix planned for 2024 would lead to lower impacts, except for EUTR. In AEW case, pH control is a relevant aspect with a direct impact on EUTR.

The results indicate that the alginate-extraction residue is a promising cadmium biosorbent and would result in interesting burden reduction in some aspects compared to a commercial material.

Acknowledgements

The authors are grateful to FAPESP (2014/05050-5) for the financial support.

Appendix A. Supplementary data

Supplementary data related to this article can be found at <https://doi.org/10.1016/j.jclepro.2018.01.025>.

References

Adebisi, G.A., Chowdhury, Z.Z., Alaba, P.A., 2017. Equilibrium, kinetic, and thermodynamic studies of lead ion and zinc ion adsorption from aqueous solution onto activated carbon prepared from palm oil mill effluent. *J. Clean. Prod.* 148, 958–968. <https://doi.org/10.1016/j.jclepro.2017.02.047>.

Åkesson, A., 2011. Cadmium exposure in the environment: renal effects and the Benchmark dose. In: *Encyclopedia of Environmental Health*. Elsevier, pp. 465–473. <https://doi.org/10.1016/B978-0-444-52272-6.00379-2>.

Aksoyoglu, S., 1989. Sorption of U(VI) on granite. *J. Radioanal. Nucl. Chem. Artic* 134, 393–403. <https://doi.org/10.1007/BF02278276>.

Asuquo, E., Martin, A., Nzerem, P., Siperstein, F., Fan, X., 2017. Adsorption of Cd(II) and Pb(II) ions from aqueous solutions using mesoporous activated carbon adsorbent: equilibrium, kinetics and characterisation studies. *J. Environ. Chem. Ecotoxicol.* 5, 679–698. <https://doi.org/10.1016/j.jece.2016.12.043>.

Baláz, M., Bujňáková, Z., Baláz, P., Zorkovská, A., Danková, Z., Briančin, J., 2015. Adsorption of cadmium(II) on waste biomaterial. *J. Colloid Interface Sci.* 454, 121–133. <https://doi.org/10.1016/j.jcis.2015.03.046>.

Barwick, M., Maher, W., 2003. Biotransference and biomagnification of selenium copper, cadmium, zinc, arsenic and lead in a temperate seagrass ecosystem from Lake Macquarie Estuary, NSW, Australia. *Mar. Environ. Res.* 56, 471–502. [https://doi.org/10.1016/S0141-1136\(03\)00028-X](https://doi.org/10.1016/S0141-1136(03)00028-X).

Basu, M., Guha, A.K., Ray, L., 2017. Adsorption behavior of cadmium on husk of lentil. *Process Saf. Environ. Protect.* 106, 11–22. <https://doi.org/10.1016/j.psep.2016.11.025>.

Ben-Ali, S., Jaouali, I., Souissi-Najar, S., Ouederni, A., 2017. Characterization and adsorption capacity of raw pomegranate peel biosorbent for copper removal. *J. Clean. Prod.* 142, 3809–3821. <https://doi.org/10.1016/j.jclepro.2016.10.081>.

Bertagnolli, C., da Silva, M.G.C., Guibal, E., 2014. Chromium biosorption using the residue of alginate extraction from *Sargassum filipendula*. *Chem. Eng. J.* 237, 362–371. <https://doi.org/10.1016/j.cej.2013.10.024>.

Blázquez, G., Martín-Lara, M.A., Tenorio, G., Calero, M., 2011. Batch biosorption of lead(II) from aqueous solutions by olive tree pruning waste: equilibrium, kinetics and thermodynamic study. *Chem. Eng. J.* 168, 170–177. <https://doi.org/10.1016/j.cej.2010.12.059>.

Boyd, G.E., Adamson, A.W., Myers, L.S., 1947. The exchange adsorption of ions from aqueous solutions by organic zeolites. II. kinetics. *J. Am. Chem. Soc.* 69, 2836–2848. <https://doi.org/10.1021/ja01203a066>.

Cantuarria, M.L., de Almeida Neto, A.F., Nascimento, E.S., Vieira, M.G.A., 2016. Adsorption of silver from aqueous solution onto pre-treated bentonite clay: complete batch system evaluation. *J. Clean. Prod.* 112, 1112–1121. <https://doi.org/10.1016/j.jclepro.2015.07.021>.

Cardoso, S.L., Costa, C.S.D., da Silva, M.G.C., Vieira, M.G.A., 2017. Dealginated seaweed waste for Zn(II) continuous removal from aqueous solution on fixed-bed column. *J. Chem. Technol. Biotechnol.* <https://doi.org/10.1002/jctb.5479>.

Cardoso, S.L., Costa, C.S.D., Nishikawa, E., da Silva, M.G.C., Vieira, M.G.A., 2017. Biosorption of toxic metals using the alginate extraction residue from the brown algae *Sargassum filipendula* as a natural ion-exchanger. *J. Clean. Prod.* 165, 491–499. <https://doi.org/10.1016/j.jclepro.2017.07.114>.

Chakravarty, P., Sarma, N.Sen, Sarma, H.P., 2010. Biosorption of cadmium(II) from aqueous solution using heartwood powder of Areca catechu. *Chem. Eng. J.* 162, 949–955. <https://doi.org/10.1016/j.cej.2010.06.048>.

Costa, C.S.D., Cardoso, S.L., Nishikawa, E., Vieira, M.G.A., Silva, M.G.C., Moino, B.P., Costa, C.S.D., Silva, M.G.C., Melissa, G., Vieira, A., 2016. Characterization of the residue from double alginate extraction from *Sargassum filipendula* seaweed. *Chem. Eng. Technol.* 52, 133–138. <https://doi.org/10.3303/CET1652023>.

Cruz-Rivera, E., Hay, M., 2001. Macroalgal traits and the feeding and fitness of an herbivorous amphipod: the roles of selectivity, mixing, and compensation. *Mar. Ecol. Prog. Ser.* 218.

Davis, T.A., Volesky, B., Mucci, A., 2003. A review of the biochemistry of heavy metal biosorption by brown algae. *Water Res.* 37, 4311–4330. [https://doi.org/10.1016/S0043-1354\(03\)00293-8](https://doi.org/10.1016/S0043-1354(03)00293-8).

Demiral, H., Güngör, C., 2016. Adsorption of copper(II) from aqueous solutions on activated carbon prepared from grape bagasse. *J. Clean. Prod.* 124, 103–113. <https://doi.org/10.1016/j.jclepro.2016.02.084>.

Díaz-Vázquez, L.M., Rojas-Pérez, A., Fuentes-Caraballo, M., Robles, I.V., Jena, U., Das, K.C., 2015. Demineralization of *Sargassum* spp. Macroalgae biomass: selective hydrothermal liquefaction process for Bio-oil production. *Front. Energy Res.* 3, 1–11. <https://doi.org/10.3389/fenrg.2015.00006>.

Doddiba, G., Nukaya, T., Kamioka, Y., Tanimura, Y., Fujita, T., 2009. Removal of arsenic from wastewater using iron compound: comparing two different types

- of adsorbents in the context of LCA. *Resour. Conserv. Recycl.* 53, 688–697. <https://doi.org/10.1016/j.resconrec.2009.05.002>.
- Dubin, M.M., Radushkevich, L.V., 1947. Equation of the characteristic curve of activated charcoal. *Proc. Acad. Sci. Phys. Chem.* 55, 331–333.
- Ebrahimi, A., Ehteshami, M., Dahrzama, B., 2015. Isotherm and kinetic studies for the biosorption of cadmium from aqueous solution by *Alhaji maurorum* seed. *Process Saf. Environ. Protect.* 98, 374–382. <https://doi.org/10.1016/j.psep.2015.09.013>.
- El-Bayaa, A.A., Badawy, N.A., Alkhalik, E.A., 2009. Effect of ionic strength on the adsorption of copper and chromium ions by vermiculite pure clay mineral. *J. Hazard Mater.* 170, 1204–1209. <https://doi.org/10.1016/j.jhazmat.2009.05.100>.
- El-Khaiary, M.I., 2007. Kinetics and mechanism of adsorption of methylene blue from aqueous solution by nitric-acid treated water-hyacinth. *J. Hazard Mater.* 147, 28–36. <https://doi.org/10.1016/j.jhazmat.2006.12.058>.
- EPE, Empresa de Pesquisa Energética, 2017. Balanço Energético Nacional 2017: Ano Base 2016 [WWW Document]. URL <https://ben.epe.gov.br> (accessed 10.11.17).
- EPE, Empresa de Pesquisa Energética, MME, Ministério de Minas e Energia, 2015. Plano Decenal de Expansão de Energia 2024 [WWW Document]. URL http://www.epe.gov.br/PDEE/Relatorio_Final.do.PDE_2024.pdf (accessed 10.11.17).
- Esmaili, A., Saremnia, B., Kalantari, M., 2015. Removal of mercury(II) from aqueous solutions by biosorption on the biomass of *Sargassum glaucescens* and *Gracilaria corticata*. *Arab. J. Chem.* 8, 506–511. <https://doi.org/10.1016/j.arabj.2012.01.008>.
- European Commission - Joint Research Centre - Institute for Environment and Sustainability, 2010. International Reference Life Cycle Data System (ILCD) Handbook - General Guide for Life Cycle Assessment: Detailed Guidance. <https://doi.org/10.2788/38479>.
- Fagundes-Klen, M.R., Ferri, P., Martins, T.D., Tavares, C.R.G., Silva, E.A., 2007. Equilibrium study of the binary mixture of cadmium–zinc ions biosorption by the *Sargassum filipendula* species using adsorption isotherms models and neural network. *Biochem. Eng. J.* 34, 136–146. <https://doi.org/10.1016/j.bej.2006.11.023>.
- Ghosal, P.S., Gupta, A.K., 2015. An insight into thermodynamics of adsorptive removal of fluoride by calcined Ca–Al–(NO₃) layered double hydroxide. *RSC Adv* 5, 105889–105900. <https://doi.org/10.1039/C5RA20538C>.
- Green Delta, 2015. OpenLCA [WWW Document]. URL <http://www.openlca.org> (accessed 4.6.17).
- Guinée, J.B., Gorreé, M., Heijungs, R., Huppes, G., Kleijn, R., Koning, A., de Oers, L., van Sleeswijk, A.W., Suh, S., Haes, H.A.U., de Bruijn, H., de Duijn, R., van Huijbregts, M.A.J., 2002. Handbook on Life Cycle Assessment. Operational Guide to the ISO Standards. I: LCA in Perspective. IIa: Guide. IIb: Operational Annex. III: Scientific Background, first ed. Kluwer Academic Publishers, Dordrecht. <https://doi.org/10.1007/0-306-48055-7>.
- Hall, K.R., Eagleton, L.C., Acrivos, A., Vermeulen, T., 1966. Pore- and solid-diffusion kinetics in fixed-bed adsorption under constant-pattern conditions. *Ind. Eng. Chem. Fund.* 5, 212–223. <https://doi.org/10.1021/i160018a011>.
- Ho, Y.-S., 2004. Citation review of Lagergren kinetic rate equation on adsorption reactions. *Scientometrics* 59, 171–177. <https://doi.org/10.1023/B:SCIE.0000013305.99473.cf>.
- Ho, Y., McKay, G., 1999. Pseudo-second order model for sorption processes. *Process Biochem.* 34, 451–465. [https://doi.org/10.1016/S0032-9592\(98\)00112-5](https://doi.org/10.1016/S0032-9592(98)00112-5).
- Holan, Z.R., Volesky, B., Prasetyo, I., 1993. Biosorption of cadmium by biomass of marine algae. *Biotechnol. Bioeng.* 41, 819–825. <https://doi.org/10.1002/bit.260410808>.
- Inyinbor, A.A., Adekola, F.A., Olatunji, G.A., 2016. Kinetics, isotherms and thermodynamic modeling of liquid phase adsorption of Rhodamine B dye onto *Raphia hookeri* fruit epicarp. *Water Resour. Invest.* 15, 14–27. <https://doi.org/10.1016/j.wri.2016.06.001>.
- Jain, M., Garg, V.K., Kadirvelu, K., 2009. Chromium(VI) removal from aqueous system using *Helianthus annuus* (sunflower) stem waste. *J. Hazard Mater.* 162, 365–372. <https://doi.org/10.1016/j.jhazmat.2008.05.048>.
- Kaewsarn, P., Yu, Q., 2001. Cadmium(II) removal from aqueous solutions by pre-treated biomass of marine alga *Padina* sp. *Environ. Pollut.* 112, 209–213. [https://doi.org/10.1016/S0269-7491\(00\)00114-7](https://doi.org/10.1016/S0269-7491(00)00114-7).
- Khezami, L., Capart, R., 2005. Removal of chromium(VI) from aqueous solution by activated carbons: kinetic and equilibrium studies. *J. Hazard Mater.* 123, 223–231. <https://doi.org/10.1016/j.jhazmat.2005.04.012>.
- Kleinübing, S.J., Gaia, F., Bertagnoli, C., da Silva, M.G.C., 2013. Extraction of alginate biopolymer present in marine alga *Sargassum filipendula* and bioadsorption of metallic ions. *Mater. Res.* 16, 481–488. <https://doi.org/10.1590/S1516-14392013005000013>.
- Kumar, S., Sahoo, D., 2017. A comprehensive analysis of alginate content and biochemical composition of leftover pulp from brown seaweed *Sargassum wightii*. *Algal Res.* 23, 233–239. <https://doi.org/10.1016/j.algal.2017.02.003>.
- Kurniawan, T.A., Chan, G.Y.S., Lo, W.-H., Babel, S., 2006. Physico-chemical treatment techniques for wastewater laden with heavy metals. *Chem. Eng. J.* 118, 83–98. <https://doi.org/10.1016/j.cej.2006.01.015>.
- Langmuir, I., 1918. The adsorption of gases on plane surfaces of glass, mica and platinum. *J. Am. Chem. Soc.* 40, 1361–1403. <https://doi.org/10.1021/ja02242a004>.
- Leusch, A., Volesky, B., 1995. The influence of film diffusion on cadmium biosorption by marine biomass. *J. Biotechnol.* 43, 1–10. [https://doi.org/10.1016/0168-1656\(95\)00102-7](https://doi.org/10.1016/0168-1656(95)00102-7).
- Ma, X., Cui, W., Yang, L., Yang, Y., Chen, H., Wang, K., 2015. Efficient biosorption of lead(II) and cadmium(II) ions from aqueous solutions by functionalized cell with intracellular CaCO₃ mineral scaffolds. *Bioresour. Technol.* 185, 70–78. <https://doi.org/10.1016/j.biortech.2015.02.074>.
- Macek, T., Mackova, M., 2011. Potential of biosorption technology. In: Kotrba, P., Mackova, M., Macek, T. (Eds.), *Microbial Biosorption of Metals*. Springer Netherlands, Dordrecht, pp. 7–17. https://doi.org/10.1007/978-94-007-0443-5_2.
- McCabe, W.L., Smith, J.C., Harriott, P., 2001. Unit Operations of Chemical Engineering, McGraw-Hill Chemical Engineering Series. McGraw-Hill. [https://doi.org/10.1016/0009-2509\(57\)85034-9](https://doi.org/10.1016/0009-2509(57)85034-9).
- Mchugh, D.J., 1987. Production, properties and uses of alginates. *FAO Fish. Tech. Pap.* 58–115.
- Metcalfe, L., Eddy, H.P., 2015. Tratamento de Efluentes e Recuperação de Recursos, Sed ed. McGraw Hill Brasil.
- Michalak, I., Chojnacka, K., Witek-Krowiak, A., 2013. State of the art for the biosorption process—a review. *Appl. Biochem. Biotechnol.* 170, 1389–1416. <https://doi.org/10.1007/s12010-013-0269-0>.
- Mobtaker, H.G., Kazemian, H., Namdar, M.A., Malekinejad, A., Pakzad, M.R., 2008. Ion exchange behavior of zeolites A and P synthesized using natural clinoptilolite. *Iran. J. Chem. Chem. Eng.* 27, 111–117.
- Moino, B.P., Costa, C.S.D., da Silva, M.G.C., Vieira, M.G.A., 2017. Removal of nickel ions on residue of alginate extraction from *Sargassum filipendula* seaweed in packed bed. *Can. J. Chem. Eng.* <https://doi.org/10.1002/cjce.22859>.
- Nishikawa, E., Costa, C.S.D., Silva, M.G.C., da Vieira, M.G.A., 2016. Cinética da bioadsorção de íons cádmio em resíduo da extração de alginato da alga *Sargassum filipendula*. In: XXI Congresso Brasileiro de Engenharia Química, 2016, Fortaleza-CE. Anais do XXI Congresso Brasileiro de Engenharia Química, Campinas-SP: Galoá, pp. 1–8.
- Plaza Cazón, J., Bernardelli, C., Viera, M., Donati, E., Guibal, E., 2012. Zinc and cadmium biosorption by untreated and calcium-treated *Macrocyctis pyrifera* in a batch system. *Bioresour. Technol.* 116, 195–203. <https://doi.org/10.1016/j.biortech.2012.04.014>.
- Puranik, P., Modak, J., Paknikar, K., 1999. A comparative study of the mass transfer kinetics of metal biosorption by microbial biomass. *Hydrometallurgy* 52, 189–197. [https://doi.org/10.1016/S0304-386X\(99\)00017-1](https://doi.org/10.1016/S0304-386X(99)00017-1).
- Qiu, H., Lv, L., Pan, B., Zhang, Q., Zhang, W., Zhang, Q., 2009. Critical review in adsorption kinetic models. *J. Zhejiang Univ. A* 10, 716–724. <https://doi.org/10.1631/jzus.A0820524>.
- Romero-González, M.E., Williams, C.J., Gardiner, P.H.E., 2001. Study of the mechanisms of cadmium biosorption by dealginated seaweed waste. *Environ. Sci. Technol.* 35, 3025–3030. <https://doi.org/10.1021/es991133r>.
- Ruthven, D.M., 1984. Principles of Adsorption and Adsorption Processes. Wiley-Interscience Publication, Wiley.
- Singh, K.K., Rastogi, R., Hasan, S.H., 2005. Removal of Cr(VI) from wastewater using rice bran. *J. Colloid Interface Sci.* 290, 61–68. <https://doi.org/10.1016/j.jcis.2005.04.011>.
- Tran, H.N., You, S., Chao, H., 2016. Thermodynamic parameters of cadmium adsorption onto orange peel calculated from various methods: a comparison study. *J. Environ. Chem. Ecotoxicol.* 4, 2671–2682. <https://doi.org/10.1016/j.jece.2016.05.009>.
- Tuazon, D., Corder, G.D., 2008. Life cycle assessment of seawater neutralised red mud for treatment of acid mine drainage. *Resour. Conserv. Recycl.* 52, 1307–1314. <https://doi.org/10.1016/j.resconrec.2008.07.010>.
- Vieira, D.M., da Costa, A.C.A., Henriques, C.A., Cardoso, V.L., Pessoa de Franca, F., 2007. Biosorption of lead by the brown seaweed *Sargassum filipendula* - batch and continuous pilot studies. *Electron. J. Biotechnol.* 10 <https://doi.org/10.2225/vol10-issue3-fulltext-3>, 0–0.
- Vilar, V.J.P., Botelho, C.M.S., Boaventura, R.A.R., 2006. Equilibrium and kinetic modelling of Cd(II) biosorption by algae *Gelidium* and agar extraction algal waste. *Water Res.* 40, 291–302. <https://doi.org/10.1016/j.watres.2005.11.008>.
- Volesky, B., Holan, Z.R., 1995. Biosorption of heavy metals. *Biotechnol. Prog.* 11, 235–250. <https://doi.org/10.1021/bp00033a001>.
- Volesky, B., Weber, J., Park, J.M., 2003. Continuous-flow metal biosorption in a regenerable *Sargassum* column. *Water Res.* 37, 297–306. [https://doi.org/10.1016/S0043-1354\(02\)00282-8](https://doi.org/10.1016/S0043-1354(02)00282-8).
- Weber, W.J., Morris, J.C., 1963. Kinetics of adsorption on carbon from solution. *J. Sanit. Eng. Div.* 89, 31–60.
- Wernet, G., Bauer, C., Steubing, B., Reinhard, J., Moreno-Ruiz, E., Weidema, B., 2016. The ecoinvent database version 3 (part I): overview and methodology. *Int. J. Life Cycle Assess.* 21, 1218–1230. <https://doi.org/10.1007/s11367-016-1087-8>.
- Yami, T.L., Du, J., Brunson, L.R., Chamberlain, J.F., Sabatini, D.A., Butler, E.C., 2015. Life cycle assessment of adsorbents for fluoride removal from drinking water in East Africa. *Int. J. Life Cycle Assess.* 20, 1277–1286. <https://doi.org/10.1007/s11367-015-0920-9>.
- Yang, R., Aubrecht, K.B., Ma, H., Wang, R., Grubbs, R.B., Hsiao, B.S., Chu, B., 2014. Thiol-modified cellulose nanofibrous composite membranes for chromium (VI) and lead (II) adsorption. *Polymer* 55, 1167–1176. <https://doi.org/10.1016/j.polymer.2014.01.043>.
- Yu, Y., Zhuang, Y., Wang, Z., 2001. Adsorption of water-soluble dye onto functionalized resin. *J. Colloid Interface Sci.* 242, 288–293. <https://doi.org/10.1006/jcis.2001.7780>.